24th COBEM - 2017

24th ABCM International Congress of Mechanical Engineering
December 3-8, 2017, Curitiba, PR, Brazil

COBEM-2017-2171
HOT DEFORMATION SIMULATION OF MODIFIED AISI 5120 LOW ALLOY STELL

Diego Aparecido Boschetti
University of Campinas, Department of Manufacturing and Materials, Campinas, Brazil
dg.boschetti@fem.unicamp.br

Ana Paola Villalva Braga
Institute for Technological Research, Center of Technology in Metallurgy and Materials, São Paulo, Brazil
anapaola@ipt.br

Paula Fernanda da Silva Farina
University of Campinas, Department of Manufacturing and Materials, Campinas, Brazil
paula.farina@fem.unicamp.br

Abstract. *The studies in the hot deformation for low alloy steels have been a scenario of many decades, but with many empirical results. Currently, to realize a preliminary view of the behavior in certain material submitted to efforts and work parameters by numerical simulation is indispensable. In addition, the industry needs to get a safe panorama for the hot working of metal alloys. Thus, this paper is a study of numerical simulation to predict the hot deformation behavior and data to generate processing map of a Mo-Si modified AISI 5120 steel. Initially a comparison was made between the original and modified steel in which a similarity in the hot deformation behavior was verified, both qualitative and quantitative. The study checked temperatures range (900 - 1200 ° C) and strain rates (1.0, 5.0, 10.0, 50.0 and 100.0* s^{-1}*), in which there is the softening phenomenon in material, with probability of dynamic recrystallization (DRX). With data obtained from the numerical simulation, it was possible to determine the strain rate sensitivity (m), which is the initial parameter for the construction of processing map. The values of m found were accepted for the determination of energy dissipation efficiency and instability* $(0 \le m \le 1)$*. Thus, the hot deformation behavior is stable and agrees to the construction of the processing map with laboratorial study.*

Keywords: *simulation, hot deformation, compression, steel, processing map.*

1. INTRODUCTION

With world production of 1,603 million tons in 2016, the steel has about 3,500 types that are distinguished by physical, chemical and environmental properties (World Steel Association, 2017). From this huge range, one of the materials used in engineering is the AISI 5120 (DIN 20MnCr5) low alloy steel. This steel is used for machine elements, like as gears, pistons, carbide bearings and, in the mechanical forming area, extrusion parts (Gunes, 2013). In addition, being considered a medium-quenched steel, the properties of good surface hardness, average internal tenacity and moderate strength are attributed to steel, it is necessary to have a cementation thermochemical treatment (Xu *et al.*, 2017), so it is known commercially as steel for carburizing.

One of the main capabilities that must be studied in low alloy steel is the plastic formability during hot forming processing. According to Bresciani Filho *et al.* (2011), "plastic formability can be defined as the ability of the metal, or the alloy, to be processed by plastic deformation without presenting defects or fractures in the workpiece". One of the most effective tools for identifying hot plastic formability and to control the materials microstructure is the construction of processing maps (Venugopal *et al.*, 1993). The processing map is a graphical representation of the material behavior, in terms of microstructural mechanisms and parameters imposed in processing, consisting of the superposition of energy dissipation and instability curves (Prasad *et al.*, 1997). This makes it possible to check ideal regions of hot workability of the material.

The parameters imposed, such as temperature, strain and strain rate can be observed from a numerical simulation of the study process. The objective of numerical simulation applicability in metals mechanical forming is to identify mechanisms of plastic deformation processes, such as kinematic behavior, formability limit and stress prediction, efforts and energy used in processing (Oliveira, 2003). Therefore, this work aims to generate a preliminary prospect, from numerical simulation predicting data for the hot deformation processing map construction of a modified AISI 5120 low alloy steel.

2. EXPERIMENTAL DETAILS

Industrially, the AISI 5120 steel has the chemical composition, shown in Tab. 1. Therefore, the chemical composition used in this research was modified with molybdenum (Mo) and silicon (Si), as shown in Tab. 1.

Table 1. Chemical composition of standard and modified AISI 5120 low alloy steel (wt%).

Steel	C	Si	Mn	P	S	Cr	Mo	N
AISI 5120	0.17 0.22	0.15 0.35	0.70 0.90	0.035	0.040	0.70 0.90	-	-
AISI 5120 Modified	0.21	1.12	1.86	0.023	0.018	1.45	0.21	0.0142

In this study, the hot deformation compression test simulation was applied. Numerical simulation was performed in QForm VX © software for the double-cone specimen model;, illustrated in Fig. 1. Developed by Jackson *et al.* (2000), the geometry assumes that the distribution of the hot deformation compression is more uniform throughout the model, reducing the number of tests compared to conventional tests. Furthermore, one can observe that the geometry restricts the bulging of the specimen, significantly reducing the friction between workpiece and tool.

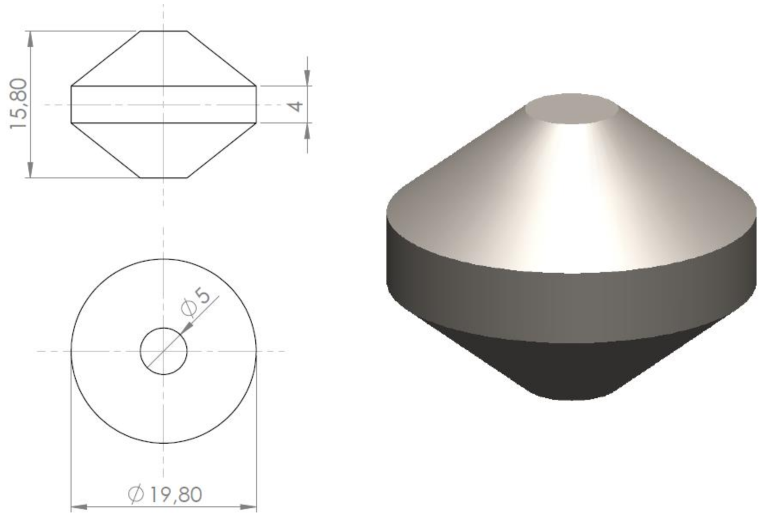

Figure 1. Geometry of the double-cone model specimen (in millimeters).

2.1 Numerical Simulation

The starting point was to compare the two materials hot work behavior. Thus, both were submitted to simulation to verify the strain, strain rate and effective stress, in order to analyze the difference of the behavior in hot deformation. The numerical simulation was performed with reduction on height of 60%, as illustrated in Fig. 2, and the hot work temperature of both materials was determined based on the no modified, 1245 °C (Chandler, 1995). The work parameters are shown in the Tab. 2.

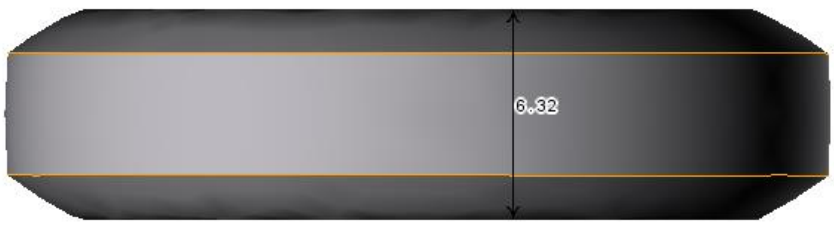

Figure 2. Model after the 60% reduction.

The mesh type used by QForm VX © software is triangular geometry, according to Fig. 3, that in which each point of the geometry (node) is an interface with another point, performing the iteration of the equations.

Table 2. Initial work parameters in numerical simulation.

Work Parameters	Values
Work	Compression
Material Temperature	1245 °C
Reduction	60%
Drive Type	Hydraulic Press
Drive Velocity	50 mm/s
Drive Load	50 MN
Tool Material	AISI D2
Tool Temperature	200 °C

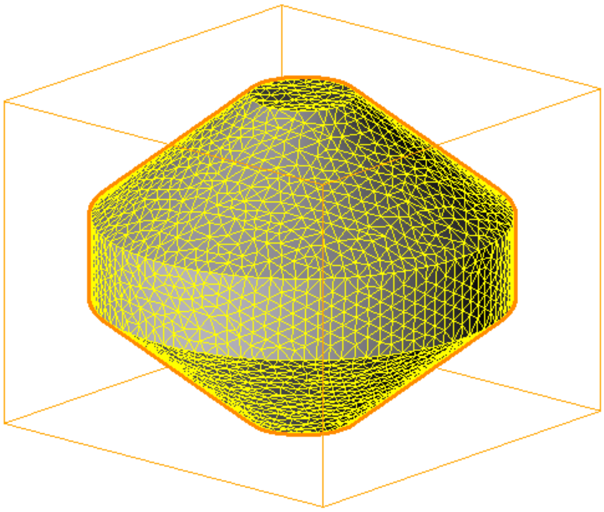

Figure 3. Triangular mesh for the numerical simulation model.

3. RESULTS AND DISCUSION

After the numerical simulation it was possible to observe in the cross section of the model that there is not significant difference in the effective stress and strain reached by the model, as shown in Fig. 4 (a) and (b). However, the strain rate showed a significant difference in values: maximum strain rate for modified material was higher (19.6782 s^{-1}) compared to the origin material (13.0453 s^{-1}); Fig. 4 (c) confirms such data showing a larger range for the modified AISI 5120 steel. Moreover, in both materials there was not rupture due to the rupture limit being 600 MPa. Thus, as it was not found a significant difference in flow matter between the two materials and assuming a larger range for the strain rate for the modified steel, it is possible to realize the simulation only with the modified AISI 5120 steel.

The numerical simulation parameters were assigned to represent the laboratory test: the hot work temperatures range of AISI 5120 steel is 870 - 1245 °C (Chandler, 1995). The temperatures determined for the numerical simulation are in the range of 900 - 1200 °C with 50 °C intervals; the numerical simulation was also performed with fixed reduction (60%) in a function of strain rates (0.01, 0.10, 1.0, 10.0 and 100.0 s^{-1}).

After performing the numerical simulations with the proposed work parameters, problems with strain rates 0.01 and 0.1 s^{-1} were noticed: in Fig. 5 (a) it is possible to see that the calculated effective stress doesn't have significant change with the alternative temperatures at strain rate of 0.01 s^{-1}, being expected a decrease in the stress with the temperature increase. Then for the strain rate 0.1 s^{-1}, Fig. 5 (b), the effective stress versus deformation curve continues to grow without a peak after a stress fall. These problems may have occurred due to some problem of calculation of the material model database in the numerical simulation software, since Puchi-Cabrera *et al.* (2014) performed simulations with AISI 5120 in deformations smaller than 1.0 s^{-1}.

In this scenario, strain rates below 1.0 s^{-1} were discarded from the study and replaced by 5.0 and 50.0 s^{-1}, obtaining the stress-strain curves of Fig. 6.

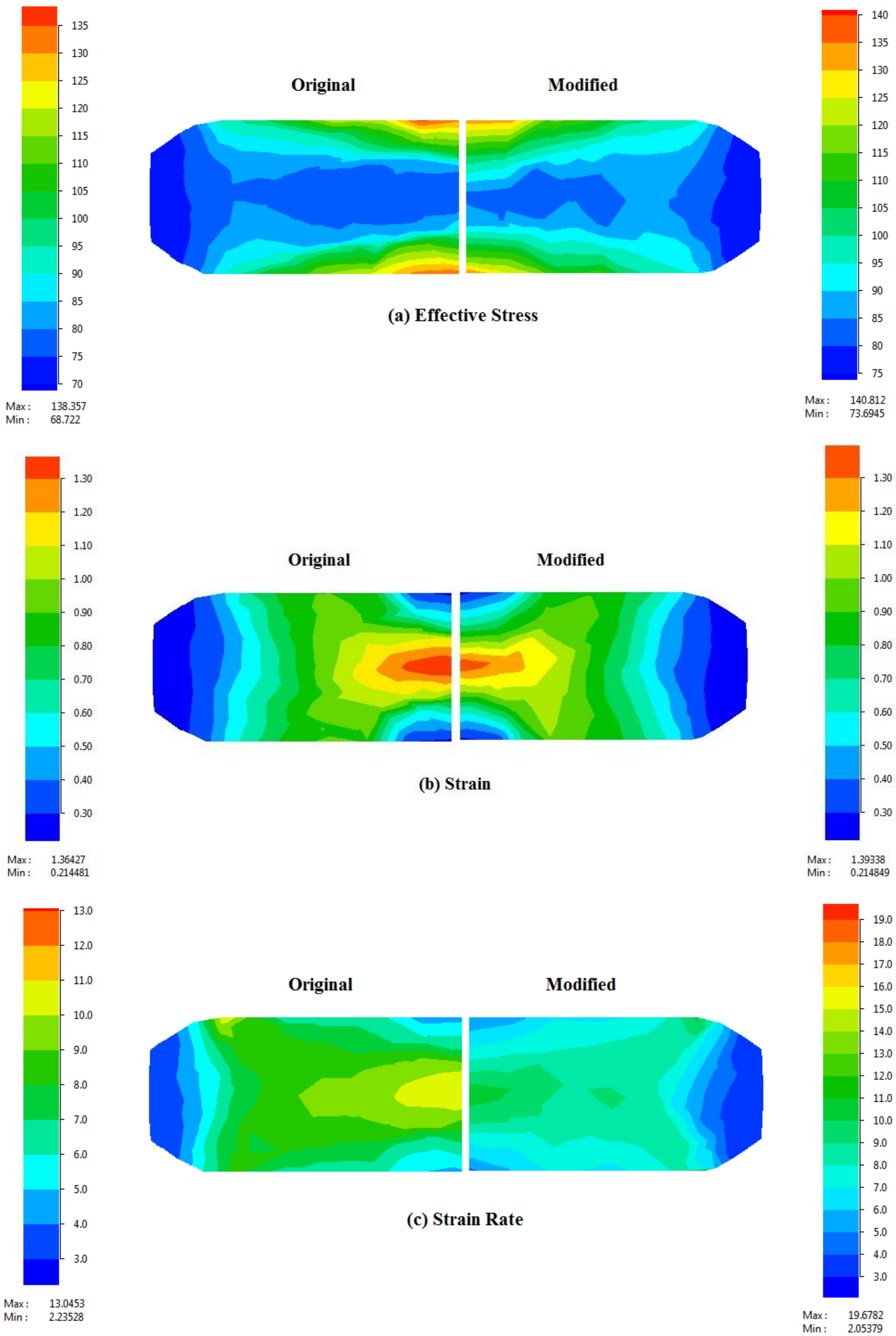

Figure 4. Initial numerical simulation results of hot deformation behavior of original and modified AISI 5120 steel: (a) effective stress, in MPa; (b) strain and (c) strain rate, in s^{-1}.

Fig. 6 shows the stress-strain curve, for the modified AISI 5120, for different temperatures and strain rates. The first analysis after the numerical simulation and obtained the stress-strain curves is to verify if the temperature increases were able to low the stress values. As shown in Fig. 6, at all simulated strain rates, the softening phenomenon occurred: in the competition between hardening versus softening, the material undergoes hardening linearly, but with the temperature factor being high, it reaches its maximum value, followed by the drop of stress, in which the softening phenomenon occurs.

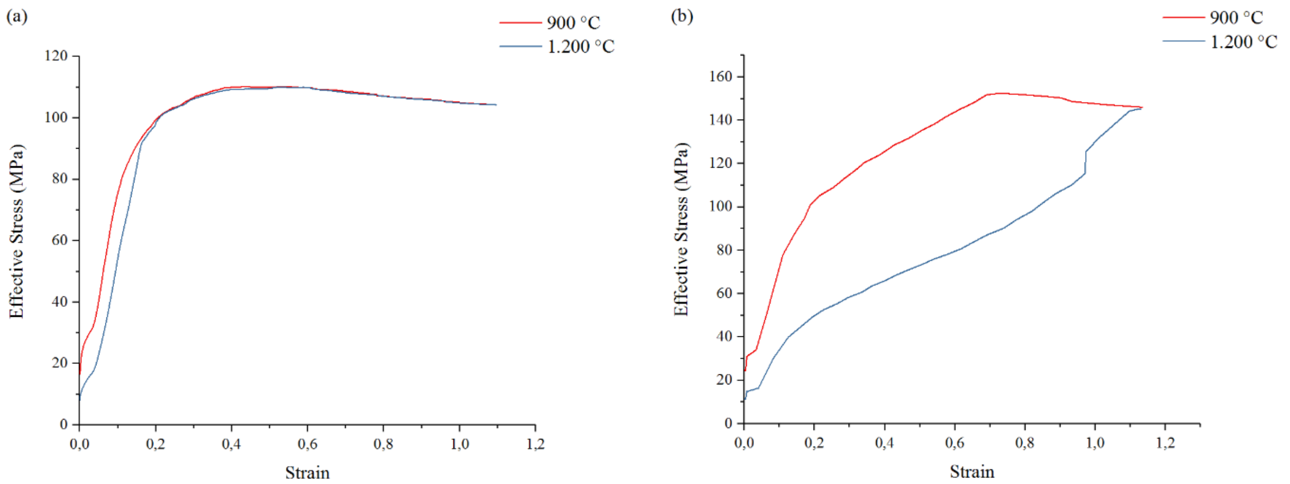

Figure 5. Stress-strain curve of modified AISI 5120: (a) 0.01 and (b) 0.1 s^{-1}.

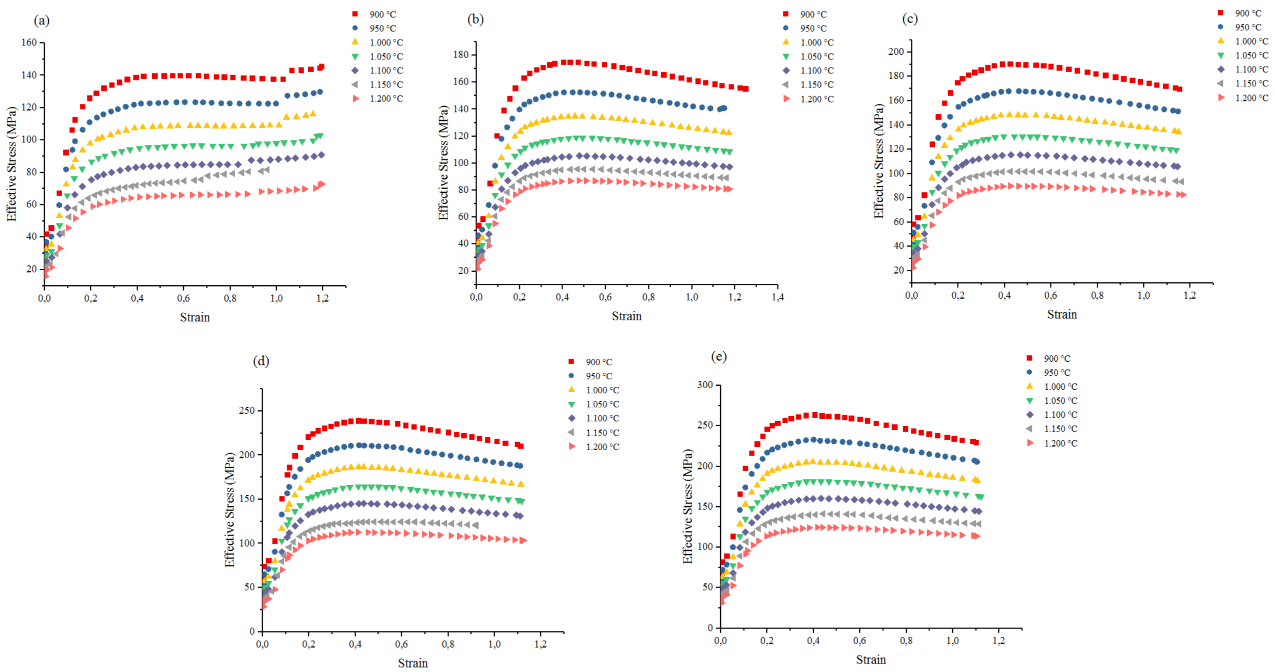

Figure 6. Stress-strain curves of modified AISI 5120: (a) 1.0, (b) 5.0, (c) 10.0, (d) 50.0 and (e) 100.0 s^{-1}.

Another important point observed is the range of stresses between the lowest temperature (900 °C) and the highest (1200 °C) for each applied strain rate: with increasing strain rates, the stresses also increased somewhat, regardless of work temperature, but at 100.0 s^{-1} the increase was much more significant, compared to the strain rate 1.0 s^{-1}, as can be seen in Tab. 3. This is also due to the material softening phenomenon: because it is at a higher temperature and with a longer soaking time, it may be being recovered and/or recrystallized dynamically, phenomena in which the stress is smaller, compared to low temperatures.

After such preliminary analyzes, it was possible to proceed with the study of the construction of processing map. Prasad *et al.* (1997) propose the Dynamic Materials Model (DMM) that uses the principle of irreversible thermodynamics with applicability in the plastic flow. The DMM is the study interface between the continuous mechanics of plastic deformation and generation of the microstructural dissipation of the material study.

Table 3. Stress range 900 - 1200 °C in function strain rate.

Strain Rate (s^{-1})	**Stress Range (900 - 1200 °C) (MPa)**
1.0	69.10
5.0	78.48
10.0	90.23
50.0	110.57
100.0	118.49

A clear way of explaining the principle of the Dynamic Materials Model is to say that the material when subjected to a certain work, dissipates energy in form of plastic deformation (G) and microstructural processes (J) (Prasad *et al.*, 1984), determining the total work energy of the material (P) (Eq. 1). The relation between these two forms of energy is the strain rate sensitivity (m).

$$P = J + G \tag{1}$$

With the increase of strain rate, in a certain strain and temperature, there is variation in the flow stress. The strain rate sensitivity (m) is the linear ratio between flow stress and strain rate, as described by Eq. (2), where T (°C) is the hot working temperature and ε is the strain applied:

$$m = \left(\frac{\partial J}{\partial G}\right) = \left(\frac{\partial \ln \sigma}{\partial \ln \dot{\varepsilon}}\right)_{T,\varepsilon} \cong \left(\frac{\Delta \log \sigma}{\Delta \log \dot{\varepsilon}}\right)_{T,\varepsilon} \tag{2}$$

With the strain rate sensitivity, it is also possible to calculate the dynamic constitutive equation. As shown in Eq. (3), the instantaneous flow stress (σ) is equated by the area at a given moment (A), strain rate for work ($\dot{\varepsilon}$) and strain rate sensitivity (m).

$$\sigma = A \cdot \dot{\varepsilon}^m \tag{3}$$

In addition to being an essential data in hot deformation of metallic materials, the strain rate sensitivity makes it possible to define the primordial parameters for the elaboration of processing maps: the energy dissipation efficiency (η) and the instability (ξ). The energy dissipation efficiency is studied from the metallurgical processes during plastic deformation (Eq. 4) and the instability analyzes the regions probable fractures and defects in material (Eq. 5), where $\xi > 0$. Both parameters must be used simultaneously for the composition of processing map, overlapping the two generated maps, η and ξ.

$$\eta = \frac{J}{J_{máx}} = \frac{2m}{m+1} \tag{4}$$

$$\xi = \frac{\partial \ln\left(\frac{m}{1+m}\right)}{\partial \ln \dot{\varepsilon}} + m < 0 \tag{5}$$

In a sense, the strain rate sensitivity is the initial parameter for the calculation of energy dissipation efficiency and instability. Thus, all the iterations between strain rate and temperature performed in numerical simulation with fixed reduction of 60% on the model, it was possible to obtain from the strain-strain curves the Tab. 4, where for 1.0 strain (maximum common value for all iterations) the following stresses were obtained:

Table 4. Stress (MPa) in 1.0 strain.

Strain Rate	**Temperatures (°C)**						
(s^{-1})	**900**	**950**	**1000**	**1050**	**1100**	**1150**	**1200**
1.0	137.74	127.46	109.10	98.39	88.13	81.74	68.64
5.0	160.93	142.18	125.49	111.18	99.30	90.63	82.45
10.0	174.51	155.09	137.70	122.14	107.89	95.54	84.29
50.0	215.78	190.85	169.19	150.66	133.75	120.33	105.21
100.0	234.18	210.55	184.81	166.22	147.39	130.55	115.69

From Tab. 4 it is possible to obtain the linear relation (Eq. 2) between ln (σ) and ln ($\dot{\varepsilon}$): for a given temperature and strain, it is possible to obtain the strain rate sensitivity (m) from a graph. Murty *et al.* (2005) studied that m changes in more complex alloys, such as stainless steel.

Therefore, the flow stress doesn't follow exactly the Energy Conservation Principle, it is necessary to use another equation for η. So, to be possible and plausible to construct the processing map, m has to satisfy the following statement: $0 \leq m \leq 1$.

If m = 0, the dissipation by microstructural processes (J) doesn't exist, so if m = 1, half of the energy is dissipated in the material flow and the other half is dissipated in heat, such as occurs in superplasticity. The Fig. 7 shows the linear relation between ln (σ) and ln ($\dot{\varepsilon}$).

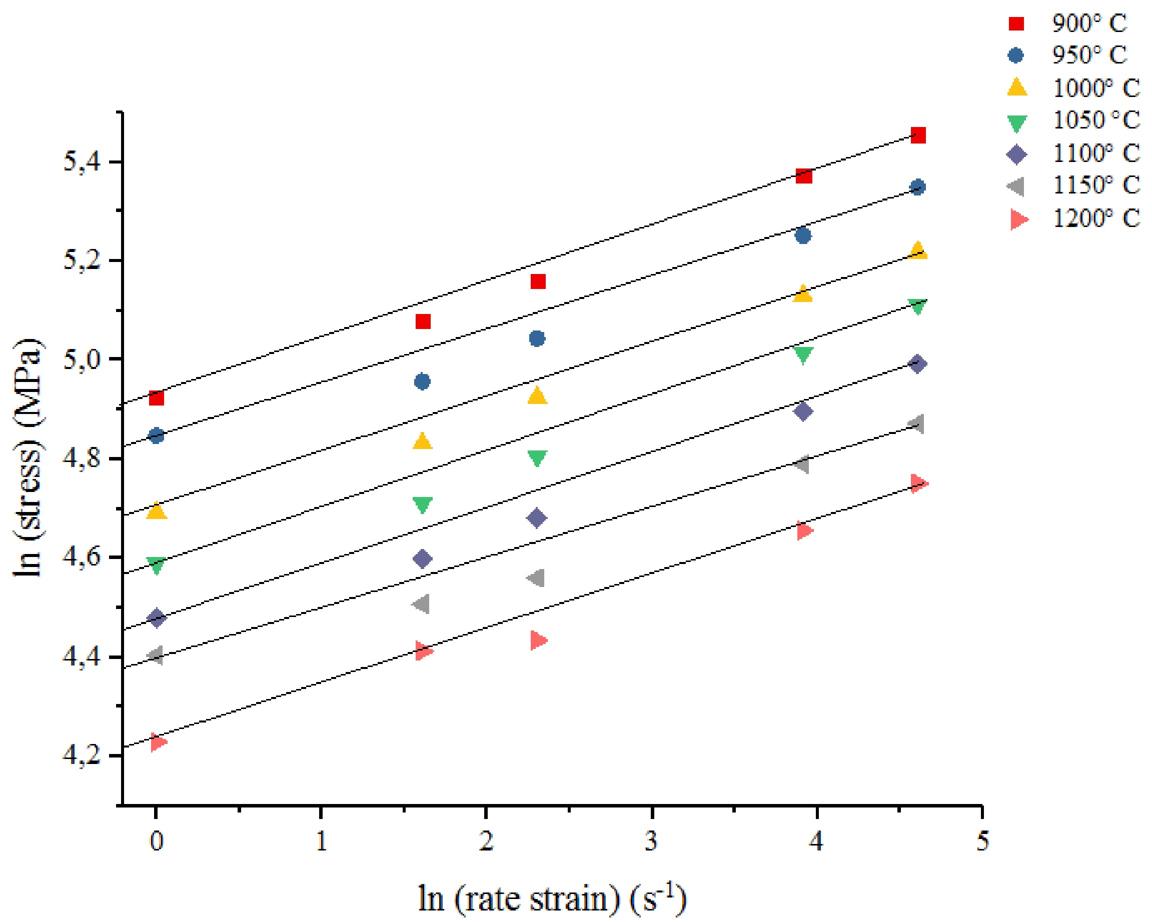

Figure 7. Linear relation between ln (σ) and ln ($\dot{\varepsilon}$).

The strain rate sensitivity (m) was calculated from Fig. 7 with the rationale of Eq. 2, where for each hot work temperature a value of m is obtained; this is observed in Tab. 5.

Table 5. Values of m found for the numerical simulation temperatures.

Temperature (°C)	m
900	0.115
950	0.109
1000	0.114
1050	0.114
1100	0.112
1150	0.102
1200	0.113

4. CONCLUSIONS

From the obtained results it is possible to conclude:

1. The numerical simulation asserts that the hot deformation behavior of AISI 5120 low alloy steel, for all applied temperatures and strain rates, is stable. For both compositions, original and modified, the stability concept has not reached the rupture limit of the material in study.
2. In the initial simulation, in which a qualitative and quantitative comparison of the two compositions of the AISI 5120 steel was performed, it was noticed that the effective stresses and strains values are not divergent from one another, but in the modified steel, it is possible to work with higher strain rates.
3. In the strain rates of 0.01 and 0.1 s^{-1}, applied initially, it was not possible to obtain stable curves and values. This may have occurred due to some erroneous iteration in software for the reason of work at low strain rates.
4. The model shows that there is the softening phenomenon in modified AISI 5120 steel at all temperatures and strain rates. The original steel has the characteristic to be a material with low stacking fault energy (SFE) and the addition of alloying elements in the has the effect of lowering further SFE. Materials with low SFE and high strain are prone to the recrystallization phenomenon, not recovery. In this case, there is not how to predict and verify the microstructure after hot work, it is safe to affirm that there is a possibility of dynamic recrystallization (DRX), but the assertion can only be plausible by laboratory test.
5. Another objective of this work was to verify the possibility of processing map construction. In the determined temperature range, the values of strain rate sensitivity (m) were close and linearity too, as shown in Fig. 7 and Tab. 5, and all values obtained are acceptable for the determination of energy dissipation efficiency and instability ($0 \leq m \leq 1$).

From all these conclusions it can be stated that the modified AISI 5120 steel has a stable behavior in the hot deformation and it is appropriate to construct the material processing map from a laboratory test with 60% height reduction and iteration of temperatures and strain rates studied.

It is important to warn the construction of a processing map is only considered real when the stress-strain curves are surveyed from a laboratory test, because the confirmation of stable and unstable domains is by microstructural analysis. The numerical simulation helps to define the possibilities of behavior when the material is subjected to hot work.

5. ACKNOWLEDGMENTS

This work was supported by University of Campinas in School of Mechanical Engineer and Institute for Technological Research in Center of Technology in Metallurgy and Materials.

Acknowledgments also to Prof. Ms. Dr. Sérgio Tonini Button for support and understanding in this present paper.

6. REFERENCES

Chandler, H., 1995. *Heat Treater's Guide: Practices and Procedures for Irons and Steels*. ASM International, Ohio, 2nd edition.

Bresciani Filho, E., Silva, I.B., Batalha, G.F. and Button, S.G., 2011. *Conformação plástica dos metais*. Editora da Unicamp, Campinas, 6th edition.

Gunes, I., 2014 "Investigation of tribological properties and characterization of borided AISI 420 and AISI 5120 steels". *Trans Indian Inst Met*, 67(3), p. 359–365.

Jackson, M., Dashwood, R.J., Christodoulou, L. and Flower, H.M., 2000. "Application of novel technique to examine thermomechanical processing of near B alloy Ti-10V-2Fe-3Al". *Materials Science and Technology*, Vol. 16 , p. 1437-1444.

Oliveira, S.A.G., 2003. "Simulação numérica de processos de conformação mecânica". In *13th POSMEC - Simpósio do Programa de Pós-Graduação em Engenharia Mecânica*. Uberlândia, Brazil.

Prasad, Y.V.R.K., Gegel, H.L., Doraivelu, S.M., Malas, J.C., Morgan, J.T., Lark, K.A. and Barker, D.R., 1984. "Modeling of dynamic material behavior in hot deformation: forging of Ti-6242". *Metallurgical Transactions*, Vol. 15ª, p. 1883-1892.

Prasad, Y.V.R.K., Rao, K.P. and Sasidhara, S., 2015. *Hot Working Guide - A compendium of processing maps*. ASM International, Ohio, 2nd edition.

Puchi-Cabrera, E.S., Guérin, J.D., Dubar M., Staia, M.H., Lesage, J. and Chicot, D., 2014. "Constitutive description for the design of hot-working operations of a 20MnCr5 steel grade". *Materials and Design*, Vol. 62, p. 255 – 264.

Venugopal, S., Mannan, S.L. and Prasad, Y.V.R.K., 1993. "Influence of cast versus wrought microstructure on the processing map for hot working of stainless steel type AISI 304". *Materials Letters*, Vol. 17, p. 388-393.

World Steel Association, 2017. "World Steel in Figures 2017". 7 Sep. 2017 < https://www.worldsteel.org/en/dam/jcr:0474d208-9108-4927-ace8-4ac5445c5df8/World+Steel+in+Figures+2017.pdf >.

Xu, Z., Wang, H., Sun, Z., Ye, Y and Tang, G., 2017. "Effect of electropulsing-assisted turning process on AISI 5120 cementation steel". *Materials Science and Technology*, Vol. 33, p. 1454-1460.

7. RESPONSIBILITY NOTICE

The author(s) is (are) the only responsible for the printed material included in this paper.